Simulation of Heavy Metals Adsorption Using Recycled Bentonite Clay Waste in a Fixed Bed Depth Column

Mukhtar DH. Abbas [1], Daryoush Yousefi Kebria [2]*

[1] Department of Environmental Engineering, Civil Engineering Faculty, Babol Noshirvani University of Technology, Iran & Engineer in Directorate of Al-Qadissiyeah Environment – Ministry of Environment, Iraq.
[2] Department of Environmental Engineering, Civil Engineering Faculty, Babol Noshirvani University of Technology, Iran.

A R T I C L E   I N F O

ORIGINAL ARTICLE

ABSTRACT

Introduction: The study objective is to remove heavy metals from an aqueous solution using recycled bentonite clay waste (RBCW) as a low-cost and green adsorbent in a continuous system. The produced RBCW results from thermal remediating of the hazardous industrial bentonite clay waste that is a by-product of used engine oil recycling plants.

Materials and Methods: The doses of the RBCW adsorbent were (1.0, 1.5, and 2.0) g mixed with (30, 40, and 50) g of the crystalline sand to produce bed depth columns of (22, 30, and 38 cm), respectively. The influent concentrations of all adsorbates were (20, 50, and 100) ppm, and the flow rates of the continuous system were (0.5, 1.0, and 2.0) mL/min.

Results: The BET, XRF, and SEM tests and the experimental data approved that RBCW is active material for heavy metals adsorption. The adsorption capacity and breakthrough time of Pb, Cd, Cr, Zn, and Ni for dominant parameters (flow rate of 1.0 mL/min, adsorbent mass of 1.0 g, and influent concentration of heavy metals of 20 ppm) were 70.36, 36.05, 27.55, 21.67, and 18.63 mg/g, and 35, 19.73, 11.38, 6.25, and 8.13 hr, respectively.

Conclusion: The RBCW adsorbent has more than one advantage in industrial and environmental issues. The (R^2) values for Thomas, Yoon-Nelson, and BDST models were higher than 0.9. Moreover, the breakthrough curves of experimental data were more fitted with the Yoon-Nelson model due to the high value of R^2 and low values of Chi-square, absolute average deviation, and standard deviation.

Introduction

In recent decades, the rapid development in industrial and agricultural activities is prominent. However, the detrimental aspect of this development is the increase in pollutants in the environmental components due to using various chemical materials in the production process[1]. According to the nature of most industrial activities, there are input materials and output of the productions in addition to the by-products.

Sometimes, the waste by-products have hazardous impacts on the environment like industrial bentonite waste resulting from used engine oil recycling plants, which was saturated with oil and impurities. They are often released into the environment without adequate remediation. The risks of bentonite waste are contamination of the surrounding soil and groundwater, and affecting living organisms due to aromatic and aliphatic hydrocarbon components that are toxic, mutagenic,

and carcinogenic[2]. The wastewater which results from industrial and agricultural activities has a high number of heavy metals. Heavy metals are toxic pollutants, non-biodegradable, prevalent, and accumulating in living organisms[3]. According to the World Health Organization (WHO), the maximum permissible limits in drinking water of Pb, Zn, Cd, Cr, and Ni are 0.01, 3.00, 0.003, 0.05, and 0.07 mg/l, respectively[4]. Different techniques have been utilized for heavy metals treatment in wastewater as electrochemical reduction, membrane filtration, chemical precipitation, and ion exchange[5]. However, low efficiency, high operational cost, and other secondary problems are vital factors in not using these methods for heavy metals treatment[6]. In the adsorption process, the dissolved species are moved from the liquid phase into the particles of the adsorbent by diffusion and then are adsorbed onto the inner surface of particles by chemical reaction or physical attraction. The advantages of the adsorption technique are low cost, flexibility in the design and operation stages, the capability of removing all contaminants even with a low concentration, ease and safety of operation, using both batch and continuous systems, no sludge formation, and regeneration of the adsorbent[7]. The adsorption processes are physical and chemical due to the nature of their characteristics. The characteristics of the physical adsorption are reversible, having low enthalpy values of about 20 kJ/mol due to weakness in the forces of the Van der Waals attraction, wear attractive, and electrostatic. Conversely, the chemical sorption is irreversible, having a high enthalpy value of about 200 kJ/mol due to stronger electrostatic forces or chemical bonds[8]. There are prominent classes of adsorbents as a natural material, industrial waste, bio-sorbent, miscellaneous sorbent, and agricultural waste[9]. Adsorbent materials that are efficient in heavy metals removal include modified bentonite clay[10, 11], activated carbon[12, 13], activated cashew nutshell[14], and waste materials (waste rock, tailings, coal ash clinker, and slag)[15].

Two well-known methods for pollutant removal from aqueous solution in the adsorption experiments are batch and continuous. The fixed bed depth is one class of continuous approaches, which is the most applicable method due to the ease in cyclic adsorption and desorption, treating a high volume of wastewater, and simplifying design and operation[16]. The fundamental parameters in the bed depth column system are flow rate, influent concentration, and bed depth of adsorbent, which are used in model building. The novelty in this work is recycling the oily industrial waste into a new, green, available, low-cost, environmentally-friendly adsorbent. The aim of this study was to investigate the maximum adsorption capacity of recycled bentonite clay waste (RBCW) to remove the heavy metals of Pb, Zn, Cd, Cr, and Ni from aqueous solution using bed depth column system with different parameters, and also analyze the experimental data and define the compatibility with the models of bed depth service time (BDST), Thomas, Yoon-Nelson, and Adam-Bohart.

Materials and Methods

Adsorbent and adsorbates

The origin of bentonite clay waste in this study is the used engine oil recycling plants drived sludge containing a high amount of engine oil. It was remediated thermally to diminish all residual oil and impurities and converted to reddish-white powder as a new adsorbent and it was called recovered bentonite clay waste (RBCW) in this study. More details of the preparation process are reported [17]. The media of the bed depth column was produced by mixing of the RBCW (1.0, 1.5, and 2.0 g) with (30, 40, and 50 g) of quartz sand at ratios of (3, 3.75, and 4%) to produce bed depth (22, 30, 38 cm), respectively. The utilized sand was rinsed with distilled water to vacate extra salt and then sieved to a desired particle size range of 0.5 and 1 mm, with three support layers of different sizes of sand at the bottom to prevent the adsorbent from escaping. The heavy metals (adsorbates) were prepared by dissolving a required quantity of the specified salts including $(ZnCl_2)$, $(PbCl_2)$, $(CdCl_2.H2O)$, $(NiCl_2.6H_2O)$, and $(CrCl_3. 6H_2O)$ in distilled water to prepare stock solutions (1000 mg/L) of (Zn, Pb, Cd, Ni, and Cr)

2079

ions. Then, the stock solutions were diluted with distilled water to prepare the demanded influent concentrations (20, 50, and 100 ppm). The salts were of analytical grade and purchased from Pan REAC. Co., Spain and the concentration of samples was investigated via flame atomic absorption spectrophotometer (SHIMADZU, AA-7000, JAPAN).

Fixed-bed adsorption experiments

The executed laboratory set-up of a fixed bed column system was in a Pyrex glass column with a length of 44 cm and 1.06 cm of internal diameter and laden with different depths of mixed adsorbents (RBCW and sand mixtures). The solution was down-flowed by gravity using the principle of constant pressure with accurate valves where all RBCW particles were immersed in the aqueous solution to ensure the adsorption process. At the bottom of the column, three supporting layers of sand with different particle sizes (small than < 0.5, 0.5 to 1, and 1.5 to 2 mm) were arranged from top to down to eliminate adsorbent loss as shown in Figure 1. The fixed bed depth was designed to adsorb heavy metals (Pb, Zn, Cd, Ni, Cr) with three parameters of depth, flow rate, and influent concentration. Then, 30, 40, and 50 g of quartz sand were mixed with 1, 2, and 3 g of RBCW to yield a total depth bed of 22, 30, and 38 cm, to avoid the occurrence of clogging, and achieve appropriate permeability of mixed bed depth[18] (Table 1). The dominant depth was 20 cm for all except the experiment of depths. The flow rates in the experiments were 0.5, 1, and 2 mL/min, and the flow rate of 1 mL/min was prevailing for all except the experiments' flow rates. The influent concentrations were 20, 50, and 100 ppm, and also 20 ppm was the dominant concentration in the other experiments. The operation was terminated when the removal efficiency became less than 5%. All experiments were accomplished at room temperature (25 ± 3ċ). It specified that the breakthrough and exhaustion time were (C_t/C_0) equal to 5% and 95%, respectively[19].

Table 1: Details of mixing process of RBCW with sand

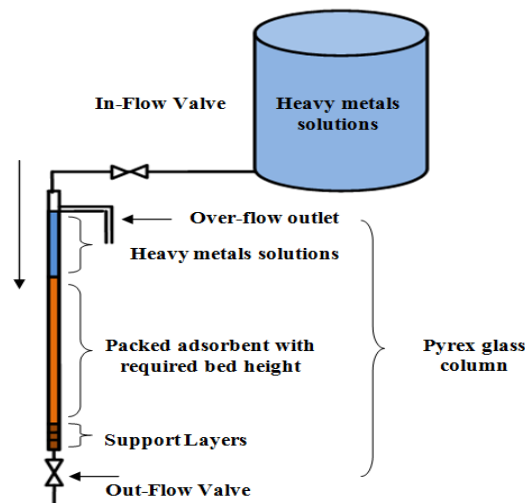| No.	Weight of RBCW (g)	Weight of sand (g)	% Ratio of (RBCW/sand)	Total bed depth column (cm)	Permeability (cm/sec)
1	1.0	30	3.33	22	0.4134
2	1.5	40	3.75	30	0.2349
3	2.0	50	4.00	38	0.1292

Figure 1: Schematic diagram of fixed bed depth column system

Study of fixed bed depth column

The breakthrough curve is a significant plot to

identify the performance of the continuous system. The plotting was between (C_t/C_0) and time. The most significant factors resulting from the breakthrough curve are breakthrough time (t_b) and exhaustion time (t_e). The (t_b) is the time compatible with concentration ratio (C_t/C_0) ranging from 1 to 10 %, in some research studies, it was reported 1% [20], 5% [21], and 10% [11]. The (t_e) is consistent with the time when (C_t/C_0) is approached (0.85- 0.95) or becomes steady. In this study, the used time was consistent with C_t/C_0 = 0.05 and 0.95 to be breakthrough time and exhaustion time, respectively. The total quantity of solutes interred in bed depth is m (mg), calculated by (Equation (1)).

$$m = C_0 * Q * t_e \qquad (1)$$

The total adsorbed quantity (q, mg) is calculated using (Equation (2))[20].

$$q = \frac{QA}{1000} = \frac{Q}{1000} \int_0^t (C_0 - C_t) dt \qquad (2)$$

Where q (mL/min) is the flow rate in the bed depth column, C_0 (mg/L) is the influent concentration, C_t (mg/L) is the effluent concentration, and A (mg.min/L) expresses the region under the breakthrough curve from (C_0) to (C_t) and from (t_0) to any (t_t).

The breakthrough capacity (q_b, mg/g) at the breakthrough point refers to the mass of molecules or ions adsorbed onto adsorbent material as written in (Equation (3)).

$$q_b = \frac{Q}{1000*w} \int_0^{t_b} (C_0 - C_t) dt \qquad (3)$$

The exhaustion capacity (q_e, mg/g) at the point of exhaustion refers to the mass of molecules or ions adsorbed onto adsorbent material according to (Equation (4)).

$$q_e = \frac{Q}{1000*w} \int_0^{t_e} (C_0 - C_t) dt \qquad (4)$$

Where t_b (min) refers to the entire time of treated effluent at the point of breakthrough, w is the adsorbent weight (g), and t_e (min) refers to the whole time of treated effluent at the exhaustion point.

The removal efficiency (R%) results from dividing the adsorbed quantity of ions qt (mg) by the total amount of solute m (mg) used in the bed depth (Equation (5)).

$$R\% = \frac{q_t}{m} \qquad (5)$$

The mass transfer zone (MTZ) (cm) is the active adsorbent region where the contaminants were adsorbed. It is dependent on the total bed depth Z (cm), the time of breakthrough and exhaustion point (Equation (6)). t_z is the required time of moving MTZ (Equation (7)) [20].

$$MTZ = Z \left(1 - \frac{t_b}{t_e}\right) \qquad (6)$$

$$t_z = t_e - t_b \qquad (7)$$

Error analysis

To demonstrate the adequacy of the BDST, Adam-Bohart, Thomas, and Yoon–Nelson model, the average absolute deviation (AAD)[22], standard deviation Δq[23], and Chi-square (x^2) tests [24] of statistical analysis were applied. These tests are non-linear approaches used to compare the experimental data and calculated model values via the excel sheets.

$$AAD = 100 * \frac{\sum \sqrt{(q_{exp.} - q_{model})^2 / q_{exp.}^2}}{NumberOfTests} \qquad (8)$$

$$\Delta q = \sqrt{\frac{\sum[(q_{exp.} - q_{model})/q_{exp.}]^2}{Number\ of\ Tests - 1}} * 100 \qquad (9)$$

$$X^2 = \frac{(q_{exp.} - q_{model})^2}{q_{model}} \qquad (10)$$

Ethical issues

The research was performed in accordance with the ethical guidelines of the Babol Noshirvani University of Technology.

Results

Characterization of the RBCW adsorbent

From the results of XRF, BET, and SEM tests, it was apparent that the characterizations of RBCW materials were promising as a new adsorbent to remove the heavy metals from aqueous solution, including ravines, excavations, and pores in the texture as shown in Figure 2. These are significant factors in increasing the adsorption process as soon

as the particle size was arranged from 21.08 to 37.17 nm. Also, the BET test approved that the specific surface area, pore size, and pore volume are positive indicators for the adsorption and are equal to 67.17 m²/g, 8.54 nm, and 0.15 cm³/g, respectively. pH_{pzc} of the RBCW adsorbent was 10.4, and this value is alkaline and assists in the sedimentation of the heavy metals and increases

the removal efficiency. In the XRF test illustrating the chemical components of the RBCW adsorbent, the elements of AL, Mg, and Ca increased from the cationic exchange with existing heavy metals in the liquid phase and then contributed to the adsorption process[18]. It was approved that the RBCW adsorbent is eco-friendly as shown in Table 2 .

Table 2: Chemical and physical characteristics of RBCW

Characteristics	Value	XRF analysis	
		Chemical composition	Weight %
Specific surface area m²/g	67.17	SiO_2	77.342
External surface area (m²/g)	77.29	Al_2O_3	10.177
Total pore volume (cm³/g)	0.15	CaO	5.443
Pore size (nm)	8.54	Mg O	3.396
pH_{PZC}	10.4	Fe_2O_3	1.112
Real density (g/cm³)	2.133	SO_3	1.11
Bulk density (g/cm³)	0.768	K_2O	0.913
CEC (meq)	22.9	Na_2O	0.201
Color	Reddish-white	TiO_2	0.097
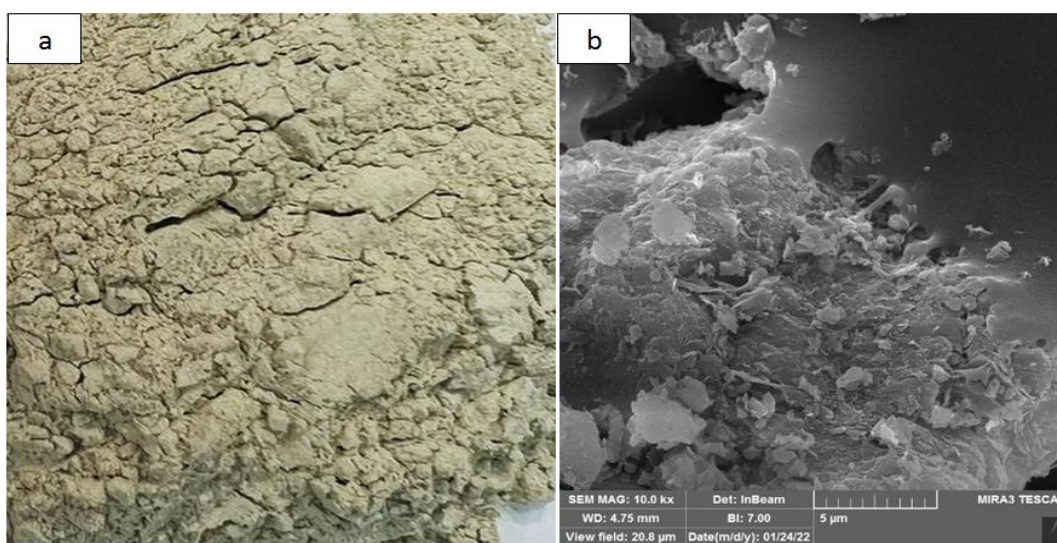
Figure 2: (a) Image of RBCW sample, (b) SEM test of RBCW

Effect of adsorbent weight in the bed

To identify the effect of the variation in the weight of the RBCW adsorbent on the adsorbing of the Pb, ZN, Cd, Ni, and Cr with flow rate and influent concentrations of 1 mL/min and 20 ppm, respectively, three employed quantities of the RBCW adsorbent 1, 1.5, and 2 g to produce equivalent bed depths of 22, 30, and 38 cm, respectively. According to Table 3, by increasing

the bed depth from 22 to 38 cm, the removal capacity increased from 70.36 to 74.30, 36.05 to 72.20, 27.55 to 28.29, 26.42 to 31.00, and 18.63 to 20.99 mg/g for Pb, Cd, Cr, Zn, and Ni, respectively. The increase in the bed depth or adsorbent quantity induced high removal efficiency due to the availability of the active sites in the RBCW surface.

Table 4 shows that an increase in the bed depth

increased the time of MTZ moving (t_z), where the (t_z) increased from 41.10 to 56.48 hr, 22.85 to 41.25 hr, 19.60 to 29.25 hr, 23.42 to 34.63 hr, and 14.23 to 33.70 hr for Pb, Cd, Cr, Zn, and Ni, respectively. Generally, MTZ increased by increasing the bed depth column. However, the increase was high for Ni, medium for Cd, Zn, and Cr, and low for Pb, and these variations in the ability of the RBCW for adsorbing ions were due to the difference in the electrochemical properties of the targeted heavy metals[25]. Both the breakthrough time and exhaustion time in Figure 3 increase with the increase in the adsorbent mass or

bed depth column of the RBCW, which ultimately increases the service time of adsorption column due to available adsorption sites and additional contact time and supplying superior intra-particle phenomena [26]. The axial dispersion and axial convection are the two influential features in the bed depth column system, and the effect on the removal efficiency, service time, and the (MTZ) is noticeable. These features are affected by the increase in the bed depth column to increase the axial convection and decrease the axial dispersion[27].

Table 3: Effect of column bed depth on the adsorption capacity (mg/g) and removal efficiency (%)

H (cm)	Pb		Cd		Cr		Zn		Ni	
	$q_{exp.}$ (mg/g)	Removal efficiency (%)	$q_{exp.}$ (mg/g)	Removal efficiency (%)	$q_{exp.}$ (mg/g)	Removal efficiency (%)	$q_{exp.}$ (mg/g)	Removal efficiency (%)	$q_{exp.}$ (mg/g)	Removal efficiency (%)
22	70.36	0.77	36.05	0.71	27.55	0.74	21.67	0.61	18.63	69.42
30	72.49	0.81	39.68	0.75	27.84	0.76	23.03	0.68	19.35	69.44
38	73.49	0.83	42.24	0.78	28.29	0.77	26.22	0.71	20.99	69.45
R^2	0.956	0.980	0.991	0.989	0.984	0.956	0.949	0.914	0.951	0.971

Table 4: Effect of column bed depth on the MTZ and the moving time

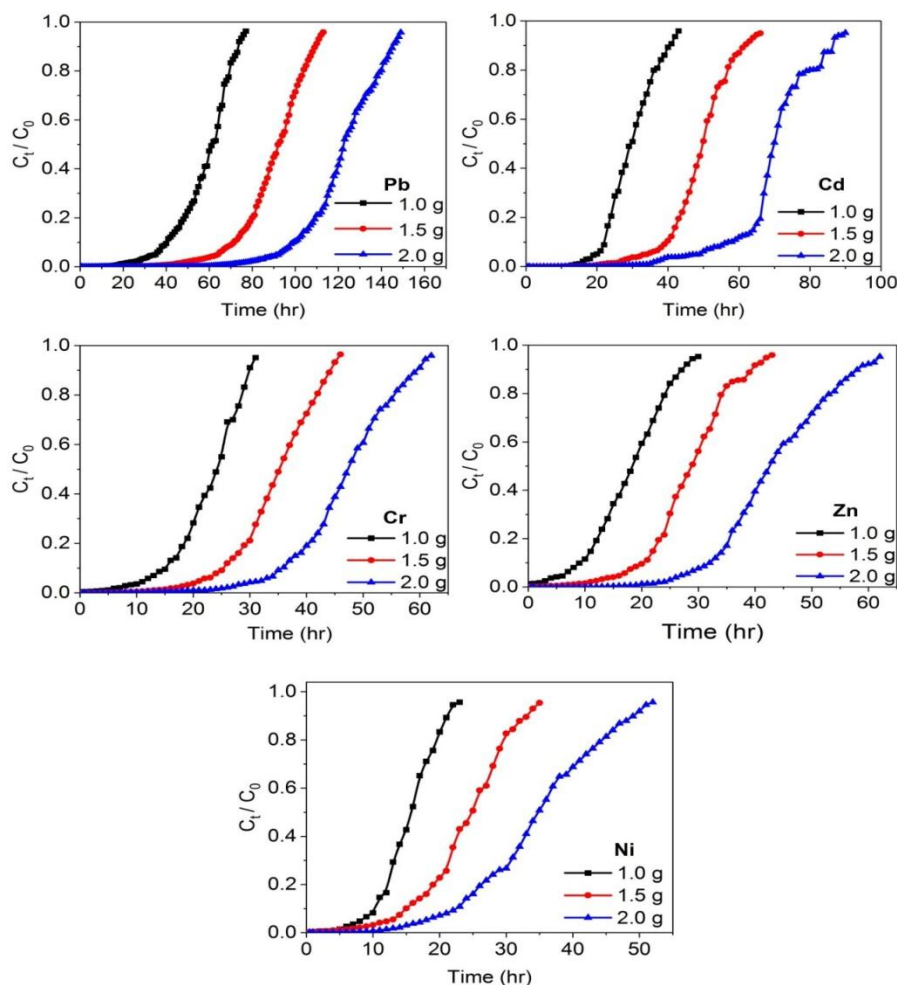| H (cm)	Pb		Cd		Cr		Zn		Ni	
	t_z (hr)	MTZ (cm)	t_z (hr)	MTZ (cm)	t_z (hr)	MTZ (cm)	t_z (hr)	MTZ (cm)	t_z (hr)	MTZ (cm)
22	41.10	11.88	22.85	11.81	19.60	13.92	23.42	17.37	14.23	14.00
30	48.22	12.89	31.90	14.51	24.32	16.02	25.82	18.38	22.43	19.32
38	56.48	14.45	41.25	17.46	29.25	18.12	34.63	21.27	33.70	24.66
R^2	0.998	0.985	1.000	0.999	1.000	1.000	0.902	0.929	0.996	1.000

Figure 3: Effect of bed depth on the breakthrough time curve for Pb, Cd, Cr, Zn, and Ni

Effect of flow rate

Three examined levels in the flow rate experiments (0.5, 1, and 2 mL/min), and influent concentration, and the bed depth column were constant at 20 ppm and 22 cm. Flow rate is a significant parameter that affects the contact time between the heavy metals (adsorbate) and the RBCW adsorbent and then determines the adsorption behavior.

Based on Table 5, the removal efficiency and the adsorption capacity declined with the increase of flow rate from 0.5 to 2 mL/min, where the adsorption capacity decreased from 75.90 to 58.87, 40.40 to 32.54, 30.14 to 19.98, 29.19 to 23.15, and 19.54 to 16.43 mg/g for Pb, Cd, Cr, Zn, and Ni, respectively. Table 6 shows that increasing the flow rate increases the height of MTZ and reduces

the time of moving (t_z) due to decreasing the breakthrough and exhaustion times. Figure 4 reveals the effect of the flow rate on the breakthrough curves, and it was evident that increasing the flow rate reduces the times of breakthrough and exhaustion to shorten the service time.

The low flow rate means an increase in the contact time, and subsequently, the opportunity of heavy metals to diffuse into the pores and active sites of the RBCW was more for achieving the equilibrium state between adsorbates and adsorbents. At a high flow rate, the film diffusion is more controlled than intra-particle diffusion, minimizing the adhesion of heavy metals on the RBCW adsorbent to reduce the removal efficiency [28].
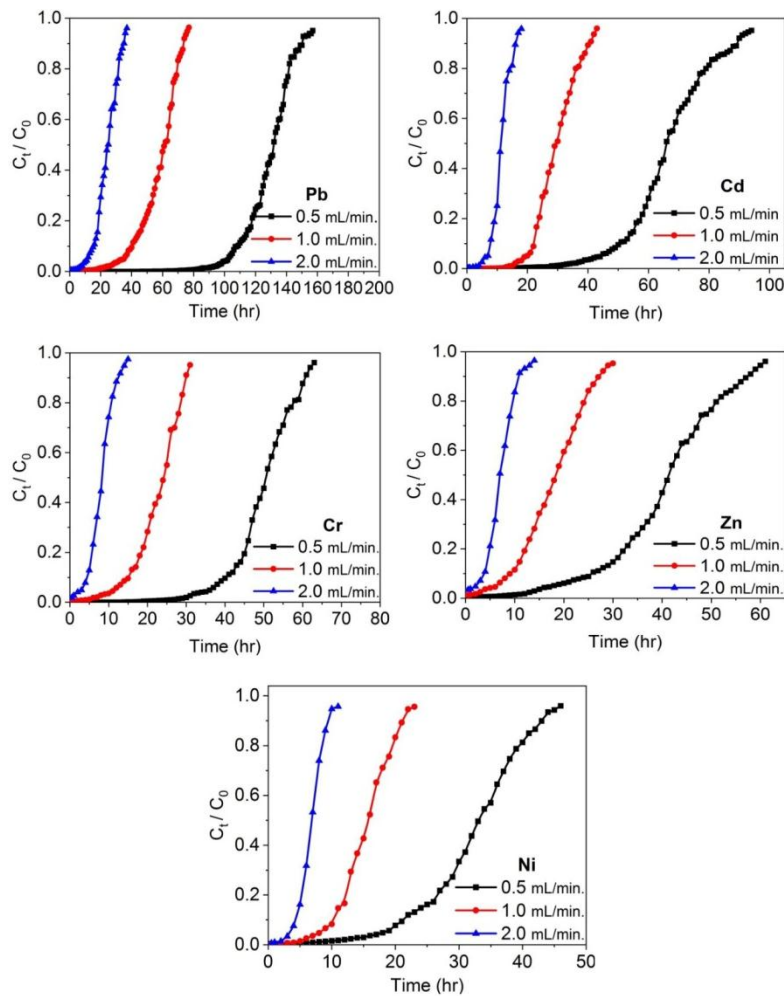
Figure4: Effect of flow rate on the breakthrough time curve for Pb, Cd, Cr, Zn, and Ni

Table 5: Effect of flow rate on the adsorption capacity (mg/g) and the removal efficiency %

Q (mL/min)	Pb		Cd		Cr		Zn		Ni	
	$q_{exp.}$ (mg/g)	Removal efficiency %	$q_{exp.}$ (mg/g)	Removal efficiency %	$q_{exp.}$ (mg/g)	Removal efficiency %	$q_{exp.}$ (mg/g)	Removal efficiency %	$q_{exp.}$ (mg/g)	Removal efficiency %
0.5	77.94	0.83	40.40	0.72	30.14	0.80	24.65	0.68	19.54	0.72
1.0	70.36	0.77	36.05	0.71	27.55	0.74	21.67	0.61	18.63	0.69
2.0	58.87	0.67	27.80	0.66	19.72	0.54	17.36	0.54	16.43	0.67
R^2	0.995	0.998	1.000	0.988	0.991	0.990	0.993	0.951	0.998	0.978

Table 6: Effect of flow rate on the MTZ and the moving time

Q (mL/min)	Pb		Cd		Cr		Zn		Ni	
	t_z (hr)	MTZ (cm)	t_z (hr)	MTZ (cm)	t_z (hr)	MTZ (cm)	t_z (hr)	MTZ (cm)	t_z (hr)	MTZ (cm)
0.5	54.52	7.64	49.50	11.62	1577	9.26	26.28	15.52	27.25	13.20
1.0	41.10	11.88	22.85	11.81	1176	13.92	19.60	17.37	14.23	14.00
2.0	24.98	15.08	10.73	13.51	731	17.61	12.18	18.53	6.87	14.74
R^2	0.981	0.928	0.848	0.941	0.975	0.936	0.903	0.901	0.883	0.955

Effect of influent concentration

The investigated influent concentrations of heavy metals (20, 50, and 100 ppm) with flow rate and bed depth column were constant at 1 mL/min and 22 cm. Table 7 shows that the increase of influent concentration from 20 to 100 ppm increased the adsorption capacity from 70.36 to 95.50 mg/g, 36.05 to 49.16 mg/g, 27.55 to 40.77 mg/g, 26.42 to 39.41 mg/g, and 18.63 to 29.77 mg/g and decreased the removal efficiency from 0.77 to 0.65 %, from 0.71 to 0.63 %, from 0.74 to 0.65 %, from 0.61 to 0.56 %, from 0.69 to 0.51 % for Pb, Cd, Cr, Zn, and Ni, respectively.

Table 8 reveals that rising influent concentration expands the MTZ and reduces the time of MTZ moving (tz). Figure 5 shows the role of influent heavy metals concentration on the breakthrough curves where it was evident that increasing the influent concentrations decreases the period times of breakthrough and exhaustion to shorten the operation service time of the column. High influent heavy metals concentration means high competition between the molecules that provide a more vital driving force[26] and an increase in the intra-particle diffusion [19] that creates significant factors in increasing the transportation of heavy metals and achieving a rapid equilibrium state of the adsorption.

Table 7: Effect of influent concentration on the adsorption capacity (mg/g) and the removal efficiency%

C_0 (mg/l)	Pb		Cd		Cr		Zn		Ni	
	$q_{exp.}$ (mg/g)	Removal efficiency %	$q_{exp.}$ (mg/g)	Removal efficiency %	$q_{exp.}$ (mg/g)	Removal efficiency %	$q_{exp.}$ (mg/g)	Removal efficiency %	$q_{exp.}$ (mg/g)	Removal efficiency %
20	70.36	0.77	36.05	0.71	27.55	0.74	21.67	0.61	18.63	0.69
50	84.87	0.69	43.22	0.66	35.17	0.68	36.48	0.58	25.29	0.58
100	95.50	0.65	49.16	0.63	40.77	0.65	48.14	0.56	29.77	0.51
R^2	0.947	0.912	0.961	0.932	0.947	0.911	0.956	0.934	0.936	0.944

Table 8: Effect of influent concentration on the MTZ and the moving time

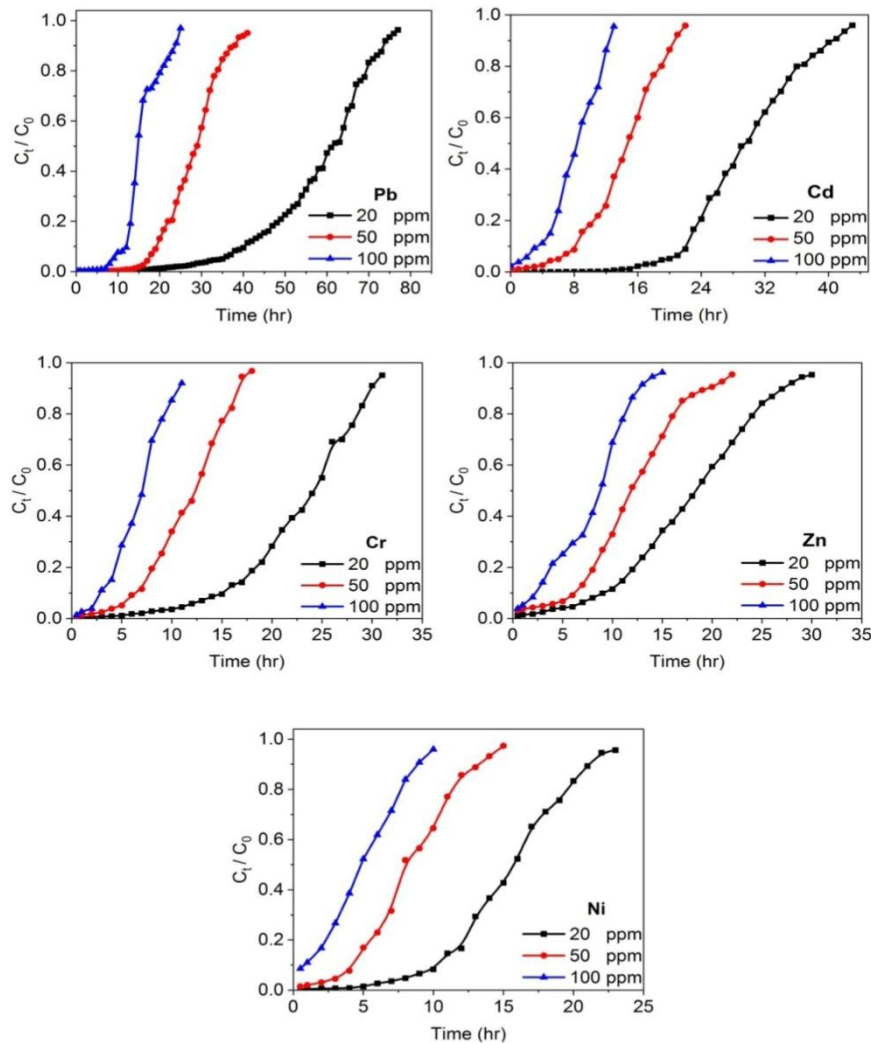| C_0 (mg/l)	Pb		Cd		Cr		Zn		Ni	
	t_z (hr)	MTZ (cm)	t_z (hr)	MTZ (cm)	t_z (hr)	MTZ (cm)	t_z (hr)	MTZ (cm)	t_z (hr)	MTZ (cm)
20	41.10	11.88	22.85	11.81	19.60	13.92	23.42	17.37	14.23	14.00
50	23.70	12.73	15.75	15.91	13.28	16.97	18.73	18.85	11.27	17.17
100	15.78	14.08	11.30	19.20	10.22	21.41	13.40	20.62	9.53	21.37
R^2	0.878	1.000	0.926	0.958	0.888	0.999	0.989	0.991	0.916	0.996

Figure5: Effect of the influent concentration on the breakthrough time curve for Pb, Cd, Cr, Zn, and Ni

Discussion

The well-known parameters that affect the adsorption process on the fixed column are the mass of the adsorbent (depth), flow rate, and influent concentration of the adsorbate; therefore, most of the experiments on the fixed bed column were conducted on these parameters. The built breakthrough curves were from the experimental data between effluent and influent concentration ratios (C_t/C_0) versus time. The most common theoretical models utilized for the adsorption process in the fixed column were Adam-Bohart, Thomas, Yoon–Nelson, and BDST. The effluent concentration, run time, and adsorption capacity can be anticipated from these models[26].

Adams–Bohart model

Adams-Bohart model is a relationship between C_t/C_0 and t in a continuous system using the surface reaction theory. It has been established for the first region of the breakthrough curve, so it is suitable for effluents at low concentrations ($C_t < 0.15C_0$)[19]. This model is a simple and comprehensive method to conduct and evaluate the adsorption process in the continuous system. It deals with presence of one adsorbate in aqueous solution without the effect of ionic form and pH on system performance.

$$ln\frac{C_t}{C_0} = K_{AB}C_0t - K_{AB}q_{AB}\frac{Z}{F} \qquad (11)$$

Where K_{AB} (L/mg.min) is the kinetic constant, F (cm/min) is the velocity of the flow, Z (cm) is the bed depth of column, and q_{AB} is the maximum adsorption capacity (mg/L).

Tables 9, 10, and 11 show the obtained results from the Adam-Bohart model for bed depth, flow rate, and influent concentration, respectively. Generally, it was apparent that an increase in the bed depth and influent concentration column increases the adsorption capacity q_{AB} (mg/l) and decreases the rate constant (K_{AB}). However, increasing the flow rate decreases the adsorption capacity and increases the rate constant (K_{AB}). Table 13 shows the difference between the experimental adsorption capacity ($q_{exp.}$) values and Adam-Bohart adsorption capacity q_{AB}, where values of linear correlation factor (R^2), AAD, Δq, and Chi-square ranged from (0.460 to 0.936), (56.67 to 19.748), (5.68 to 1.136), and (3435.93 to 1041.6), respectively for all experiments of heavy metals. The table also reveals low values of (R^2) and high value of other parameters of error analysis. The results indicated that Adams-Bohart model is less compatible with adsorption data for all heavy metals, since this model is applicable almost for the determined range of the adsorption ($C_0/C_t < 0.7$) that the kinetic adsorption depending on the physical (or external) mass transfer[18]. The adsorption constant increases with the rise of flow rate and decreases with an increase in influent concentration and bed depth column to be similar to that in[29].

Thomas model

Thomas has offered a model using the assumptions of pseudo second order kinetics and Langmuir kinetics for the breakthrough curves[19], subsequently, some researchers used it to predict the breakthrough curve of heavy metal adsorption with different adsorbent in experiments of fixed-bed column. The formula of linear Thomas model is shown below.

$$ln\left(\frac{C_0}{C_t} - 1\right) = K_{Th}q_{Th}\frac{m}{Q} - K_{Th}C_0 t \qquad (12)$$

Where K_{Th} (mL/(mg min)) is the Thomas rate constant, q_{Th} (mg/g) is the maximum adsorption capacity, C_0 and C_t (mg/L) are the influent, and effluent concentration of adsorbates, respectively, m (g) is the quantity of absorbent in the column, Q (mL/min) is the flow rate, and t (min) is the

filtration time. The plot of ln [(C_0/C_t)–1] against (t) at a specified flow rate and mass of adsorbent should produce a straight line if the measurements follow the Thomas model. The kinetic parameters of K_{Th} and q_0 can be calculated from the slope and intercept[30], and this model depends on the axial dispersion and internal mass transfer[31]. Adsorption capacity q_{Th} (mg/g) and rate constant K_{Th} (ml/mg.min) that result from applying Thomas model for different bed depth, flow rate, and influent concentration are shown in Tables 9, 10, and 11, respectively. It was apparent that increasing the bed depth and influent concentration increases the adsorption capacity due to the availability of high adsorption sites and more competition between the ions of heavy metals. However, at the same time, the rate constant (K_{Th}) decreased. Moreover, increasing the flow rate decreased the adsorption capacity due to reducing the contact time between the adsorbates and the adsorbent. However, the increase rate was constant, which was similar to the study by (Alamin. AH & Kaewsichan L)[32]. The experimental ($q_{exp.}$) values were close to the values that result from Thomas model q_{Th}, where the values of linear correlation factor (R^2), AAD, Δq, and Chi-square ranged from 0.995 to 0.998, 0.6935 to 1.2056, 0.0253 to 0.0910, and 0.0274 to 0.1899, respectively for all experiments of heavy metals as shown in Table 13.

Yoon–Nelson model

The Yoon–Nelson model is relatively simple and demands no detailed data about the properties of the adsorbate, the kind of adsorbent, and adsorption characteristics parameters. The assumption of the model is that the rate of decrease in the probability of adsorption for each molecule is proportional to the probability of adsorbate adsorption and the probability of adsorbate breakthrough on the adsorbent[24]. The linear Yoon–Nelson model can be expressed by the following equation.

$$ln\left(\frac{C_t}{C_0 - C_t}\right) = K_{YN}t - \tau K_{YN} \qquad (13)$$

Where K_{YN} (mL/(min.mg)) is the Yoon–Nelson

rate constant, τ (min)is the time required for 50% adsorbate breakthrough, and C_0 and C_t (mg/L) are the influent and effluent concentration of adsorbates, respectively (mg/L).

Parameters of Yoon-Nelson model shown in Table 9 approved that increasing the bed depth increased the values of τ and decreased K_{YN} due to a more binding site. Tables 10 and 11 explain that increasing flow rate and influent concentration

increased K_{YN} and decreased 50% of breakthrough time τ due to rapid saturation[33]. There was a slight contrast between experimental $\tau$and model τ_{YN}, where the values of linear correlation factor (R^2), AAD, Δq, and Chi-square ranged from 0.998 to 1.0, 0.6248 to 2.6715, 0.0275 to 0.100, and 0.3795 to 13.1256, respectively for all experiments of heavy metals as shown in Table 13.

Table 9: Adams–Bohart, Thomas, and Yoon–Nelson model parameters of heavy metals at different bed depths

Bed Depth (cm)	Heavy metals	$q_{exp.}$ (mg/g)	$q_{exp.}$ (mg/l)	Adams–Bohart model			Thomas model			Yoon–Nelson model		
				q_{AB} (mg/l)	K_{AB} (ml/mg.min)	R^2	q_{Th} (mg/g)	K_{Th} (ml/mg.min)	R^2	τ (Min)	τ_{exp} (Min)	K_{YN} (Min^{-1})
22		70.4	3427	4053	0.0756	0.982	70.3	0.0972	0.989	3516	3518	0.0019
30	Pb	72.5	3883	4376	0.0679	0.986	72.8	0.0808	0.995	5457	5437	0.0016
38		73.5	4144	4559	0.0627	0.989	74.1	0.0715	0.998	7407	7349	0.0014
22		36.1	1756	2080	0.2001	0.924	36.9	0.2486	0.985	1847	1803	0.0050
30	Cd	39.7	2126	2455	0.1196	0.969	39.7	0.1487	0.996	2977	2975	0.0030
38		42.2	2380	2712	0.0881	0.979	42.3	0.1068	0.991	4232	4224	0.0021
22		27.6	1342	1655	0.1538	0.983	27.7	0.2070	0.987	1384	1378	0.0041
30	Cr	27.8	1492	1747	0.1422	0.977	27.9	0.1795	0.996	2091	2088	0.0036
38		28.3	1596	3396	0.1112	0.980	28.4	0.1393	0.993	2843	2829	0.0028
22		21.7	1055	1489	0.1249	0.932	21.8	0.2028	0.998	1088	1083	0.0041
30	Zn	23.0	1234	1573	0.1267	0.959	23.2	0.1800	0.997	1738	1728	0.0036
38		26.2	1479	1762	0.1229	0.945	26.7	0.1553	0.995	2672	2622	0.0031
22		18.6	907	1158	0.2277	0.954	18.7	0.3251	0.997	934	932	0.0065
30	Ni	19.4	1037	1791	0.1396	0.969	19.4	0.1975	0.996	1452	1451	0.0040
38		21.0	1184	2552	0.1119	0.963	21.3	0.1521	0.994	2128	2099	0.0030

Table 10: Adams–Bohart, Thomas, and Yoon–Nelson model parameters of heavy metals at different flow rates

Flow Rate (cm)	Heavy metals	$q_{exp.}$ (mg/g)	$q_{exp.}$ (mg/l)	Adams–Bohart model			Thomas model			Yoon–Nelson model		
				q_{AB} (mg/l)	K_{AB} (ml/mg.min)	R^2	q_{Th} (mg/g)	K_{Th} (ml/mg.min)	R^2	τ (Min)	τ_{exp} (Min)	K_{YN} (Min^{-1})
0.5		77.9	3796	4146	0.0685	0.991	78.4	0.0777	0.997	7835	7794	0.0016
1.0	Pb	70.4	3427	4053	0.0756	0.982	70.3	0.0972	0.989	3516	3518	0.0019
2.0		58.9	2867	3701	0.1312	0.946	59.3	0.1886	0.997	1482	1472	0.0038
0.5		40.4	1967	2368	0.0723	0.970	40.9	0.0938	0.997	4088	4040	0.0019
1.0	Cd	36.1	1756	2080	0.2001	0.924	36.9	0.2486	0.985	1847	1803	0.0050
2.0		27.8	1354	1779	0.3039	0.940	28.3	0.4431	0.995	706	695	0.0089
0.5		30.1	1468	1664	0.1258	0.988	30.3	0.1504	0.994	3033	3014	0.0030
1.0	Cr	27.6	1342	1655	0.1538	0.983	27.7	0.2070	0.987	1384	1378	0.0041
2.0		19.7	960	1462	0.2400	0.916	19.8	0.4383	0.997	494	493	0.0088
0.5		24.7	1201	1536	0.0795	0.956	24.7	0.1138	0.996	2471	2465	0.0023
1.0	Zn	21.7	1055	1489	0.1249	0.932	21.8	0.2028	0.998	1088	1083	0.0041
2.0		17.4	845	1360	0.2311	0.904	17.5	0.4452	0.991	437	434	0.0089
0.5		19.5	952	1192	0.1099	0.996	19.5	0.1538	0.989	1950	1954	0.0031
1.0	Ni	18.6	907	1158	0.2277	0.954	18.7	0.3251	0.997	934	932	0.0065
2.0		16.4	800	1095	0.4387	0.936	16.5	0.6887	0.996	413	411	0.0138

Table 11: Adams–Bohart, Thomas, and Yoon–Nelson model parameters of heavy metals at different concentrations

Concentration (cm)	Metal Ions	$q_{exp.}$ (mg/g)	$q_{exp.}$ (mg/l)	Adams–Bohart model			Thomas model			Yoon–Nelson model		
				q_{AB} (mg/l)	K_{AB} (ml/mg.min)	R^2	q_{Th} (mg/g)	K_{Th} (ml/mg.min)	R^2	τ (Min)	τ_{exp} (Min)	K_{YN} (Min^{-1})
20		70.4	3426	4053	0.0756	0.982	70.3	0.0972	0.990	3516	3518	0.0019
50	Pb	84.9	4133	5002	0.0727	0.935	86.4	0.0942	0.994	1728	1697	0.0047
100		95.5	4651	6108	0.0472	0.926	99.3	0.0662	0.980	993	955	0.0066
20		36.1	1756	2080	0.2001	0.924	36.9	0.2486	0.985	1847	1803	0.0050
50	Cd	43.2	2105	2803	0.0758	0.956	43.2	0.1147	0.995	864	864	0.0057
100		49.2	2394	3418	0.0485	0.955	48.9	0.0801	0.982	489	492	0.008
20		27.6	1342	1655	0.1538	0.983	27.7	0.2070	0.987	1384	1378	0.0041
50	Cr	35.2	1713	2290	0.0921	0.948	34.8	0.1429	0.988	696	703	0.0071
100		40.8	1985	2795	0.0660	0.912	41.4	0.1030	0.981	414	408	0.1030
20		21.7	1055	1489	0.1249	0.932	21.8	0.2028	0.998	1088	1083	0.0041
50	Zn	36.5	1776	2714	0.0590	0.924	36.8	0.1048	0.993	637	730	0.0052
100		48.1	2344	3771	0.0356	0.918	47.1	0.0711	0.986	471	481	0.0071
20		18.6	907	1158	0.2277	0.954	18.7	0.3251	0.997	934	932	0.0065
50	Ni	25.3	1232	1751	0.1075	0.920	25.8	0.1700	0.995	517	506	0.0085
100		29.8	1450	2560	0.0428	0.923	29.2	0.0926	0.994	292	298	0.0093

The BDST model

The BDST model was applied to estimate the design parameters such as bed depth and breakthrough time (t_b) of fixed-bed column. This model was revised by Hudchins from the Bohart-Adams model, stating that molecules are directly adsorbed onto the adsorbent surface and the forces of intra-particle diffusion and external mass transfer are negligible[24].

$$t_b = \frac{N_0}{C_0 U_0} Z - \frac{1}{K_0 C_0} Ln\left(\frac{C_0}{C_t} - 1\right) \qquad (14)$$

Where t (min) is the breakthrough time of bed column, Z (cm) is the bed depth of adsorbent, N_0 (mg/L) is the column adsorption capacity, K_0 [L/(mg.min)] is the rate constant, C_0 (mg/L) is the influent concentration, C_t (mg/L) is the effluent concentration, and U_0 (cm/min) is the linear flow velocity.

At three different experimental conditions, bed depths, flow rates, and influent adsorbent concentration were investigated to determine the model parameters (rate constant, K_0 and adsorption capacity, N_0). Figure 6 explains the relationship between the service time and bed depth of column for breakthrough time (t_b) and exhaustion time (t_e) with R^2 values ranging > 0.998, > 0.997, > 0.999, > 0.983, and > 0.999 for Pb, Cd, Cr, Zn, and Ni, respectively.

Table 12 shows the values of experimental adsorption capacity q_{exp}, modeling adsorption capacity N_0, the rate constant K_0, and R^2 that result from the BDST model. It approved that increasing bed depth and influent concentration increase the adsorption capacity N_0 and decrease the rate constant K_0. In contrast, an increase in flow rate decreased the adsorption capacity and increased the rate constant K_0. These results of modeling are consistent with the study by (Kapur. M & Mondal. MK) [34]. Table 12 shows that the BDST model was compatible to the experimental value where the values of linear correlation factor (R^2), AAD, Δq, and Chi-square ranged from 0.9947 to 0.998, 0.6353 to 2.6716, 0.0261 to 0.2280, and 0.8506 to 28.9217, respectively for all experiments of heavy metals.

Finally, the rank of the applied models was Yoon-Nelson > Thomas > BDST, where all values of R^2 were more than 0.9, and the most suitable model for experimental data was the Yoon-Nelson model, since Table 13 displays that it has the highest R^2 value and lowest values of deviation. The Adam-Bohart was the least suitable model because it was suitable only for the determined range of the C_0/C_t and was equal to or less than < 0.7 in this study.
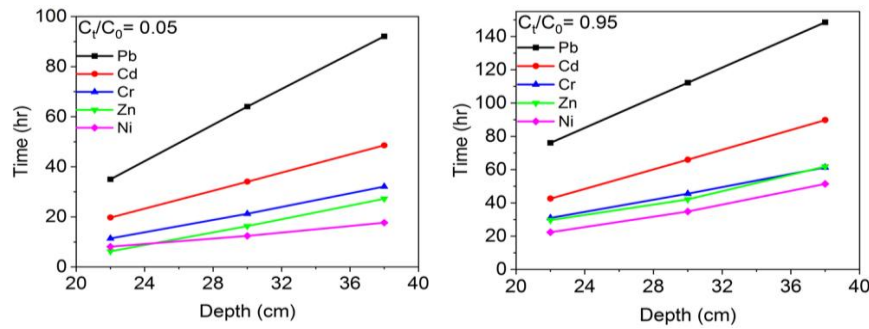
Figure6: The time of breakthrough point and exhaustion obtained from BDST model

Table 12: BDST model parameters of heavy metals at different bed depths, flow rates, and concentrations

Heavy metals	Experimental conditions							
	Bed depth (cm)	22	30	38	22	22	22	22
	Influentconcentration (ppm)	20	20	20	20	20	50	100
	Flow rate (ml/min)	1.0	1.0	1.0	0.5	2.0	1.0	1.0
	BDST model parameters							
Pb	$q_{exp.}$ (mg/l)	3246	3883	4144	3796	2867	4133	4651
	N_0 (mg/l)	3425	3898	4177	3816	2887	4208	4836
	K_0 (ml/mg.min)	0.097	0.081	0.072	0.078	0.189	0.094	0.066
	R^2	0.990	0.995	0.998	0.997	0.997	0.994	0.980
Cd	$q_{exp.}$ (mg/l)	1756	2125	2382	1967	1354	2105	2394
	N_0 (mg/l)	1799	2126	2386	1991	1376	2104	2383
	K_0 (ml/mg.min)	0.249	0.149	0.107	0.094	0.443	0.115	0.080
	R^2	0.985	0.996	0.990	0.997	0.995	0.995	0.982
Cr	$q_{exp.}$ (mg/l)	1342	1492	1596	1468	960	1713	1985
	N_0 (mg/l)	1348	1494	1603	1477	962	1694	2018
	K_0 (ml/mg.min)	0.207	0.179	0.139	0.150	0.438	0.143	0.103
	R^2	0.987	0.996	0.993	0.997	0.997	0.988	0.992
Zn	$q_{exp.}$ (mg/l)	1055	1234	1479	1201	846	1776	2344
	N_0 (mg/l)	1060	1242	1507	1203	851	1794	2293
	K_0 (ml/mg.min)	0.203	0.180	0.155	0.114	0.445	0.105	0.071
	R^2	0.998	0.997	0.995	0.996	0.991	0.993	0.986
Ni	$q_{exp.}$ (mg/l)	907	1037	1184	952	800	1232	1450
	N_0 (mg/l)	909	1037	1200	950	804	1258	1423
	K_0 (ml/mg.min)	0.325	0.198	0.152	0.154	0.689	0.170	0.093
	R^2	0.997	0.996	0.994	0.989	0.996	0.995	0.994

Table 13: Results of error analysis for Adams–Bohart, Thomas, Yoon–Nelson, and BDST models

Parameters	Adam-Bohart					Thomas				
	Pb	**Cd**	**Zn**	**Cr**	**Ni**	**Pb**	**Cd**	**Zn**	**Cr**	**Ni**
AAD	19.748	25.083	41.468	41.904	56.669	1.206	0.871	0.959	0.694	0.938
Δq	1.211	1.136	2.165	4.753	5.687	0.038	0.091	0.091	0.025	0.062
Chi-square	1218.81	1041.61	2097.28	2960.22	3435.93	0.19	0.035	0.036	0.016	0.027
R^2	0.792	0.794	0.936	0.460	0.7684	0.997	0.998	0.999	0.998	0.995

Parameters	Yoon-Nelson					BDST				
	Pb	**Cd**	**Zn**	**Cr**	**Ni**	**Pb**	**Cd**	**Zn**	**Cr**	**Ni**
AAD	1.175	0.868	2.672	0.625	0.935	2.672	1.035	1.039	0.635	0.895
Δq	0.036	0.100	0.0835	0.027	0.057	0.228	0.100	0.084	0.026	0.056
Chi-square	2.894	1.853	13.126	0.379	0.784	28.922	2.522	1.951	0.851	1.297
R^2	1.000	0.999	0.999	1.000	0.999	0.985	0.998	0.998	0.998	0.995

Comparison of adsorption capacity

Remediating the industrial solid waste and recycling to adsorbent materials for the removal of heavy metals should possess several specifications, including effective for the adsorption of a broad number of heavy metals, low cost, easily disposed of after adsorption or regeneration, and eco-friendly.

There is no study utilizing oily industrial solid waste as a green and new adsorbent, and the RBCW was more available, cost-effective, eco-friendly, and had high adsorption capacity compared to the determined conventional adsorbents in Table 14. It was approved that RBCW is sufficient as a novel adsorbent to remove the heavy metals via the fixed bed depth column system.

Table 14: Previous studies for comparison according to the adsorption capacity

Adsorbent	Adsorbate	Flow rate (ml/min)	Bed depth (cm)	Influent concentration (ppm)	Diameter of column (cm^2)	Adsorbent mass (g)	qm (mg/g)	Reference
Modified beer lees	Pb (II) Zn (II)	1	-----	30 15	-----	4	29.6 5.43	(26)
Calcined clay	Pb (II) Cd (II) Cr (II)	5.6	4	100	1.5	-----	28.6 21.4 14.2	(35)
PAMAM/CNT nanocomposite*	Zn (II)	3	12	100	-----	-----	462	(36)
Modified A. barbadensis Miller leaves	Ni (II)	10	6	20	2	3	14.4	(37)
Waste tea factory	Ni (II)	10	30	100	2	10.5	13.6	(38)
Dead calcareous skeletons	Cd (II) Pb (II)	10	1.1	100	4.4	20	20.5 44.1	(39)
RBCW	Pb (II) Cd (II) Cr (II) Zn (II) Ni (II)	1	-----	20	1.1	1	70.4 36.1 27.6 21.7 18.6	This study

*- Carbon Nanotubes (CNTs) coated Poly amidoaminedendrimer (PAMAM).

Conclusion

In this study, recycling of bentonite waste as a low-cost adsorbent for removing the heavy metals from an aqueous solution has advantages on the industrial and environmental issues. From the experimental results of RBCW characteristics and heavy metal adsorption in the bed depth column system, it can be concluded that

1- The RBCW can be utilized in the practical application of industrial wastewater treatment by batch and dynamic flow methods with a wide range of parameters, influent concentration, flow rate, and bed depth that have a role in the adsorption capacity.

2- Increasing bed depth increases adsorption capacity, removal efficiency, surface time, and MTZ. Increasing influent concentration increases adsorption capacity and MTZ and decreases removal efficiency and surface time. Increasing flow rate increases MTZ and decreases adsorption capacity, removal efficiency, and surface time.

3- The adsorption capacity of dominant parameters, flow rate, influent concentration, and depth bed (1 mL/min, 20 ppm, and 22 cm) for Pb, Cd, Cr, Zn, and Ni are 70.36, 36.05, 27.55, 21.67 and 18.63 mg/g, respectively.

4- The adsorption on the RBCW surface was more for Pb ion and less for Ni ion due to the electrochemical properties such as ionic radius, softness value, and hydration energy.

5-The coefficient of determination (R^2) of breakthrough curves of Adams-Bohart was less than < 0.9, while for other models was more than > 0.9, and the Yoon-Nelson model was more compatible with experimental data due to higher R^2 and low deviation. The rank of models was Yoon-Nelson > Thomas > BDST >Adams-Bohart.

Conflict of interest

The authors declare that they have no conflict of interest.

References

1. Waisi BI, Arena JT, Benes NE, et al. Activated carbon nanofiber nonwoven for removal of emulsified oil from water. Microporous Mesoporous Mater. 2020;296:109966.

2. Jaber W. Sorption of engine oil from aqueous solution into ricinus communis leaves in three-phase fluidized bed reactor [Thesis]. Iraq: Baghdad; 2020.

3. Saleh TA, Gupta VK, Al-Saadi AA. Adsorption of lead ions from aqueous solution using porous carbon derived from rubber tires: experimental and computational study. J Colloid Interface Sci. 2013;396:264-9.

4. WHO. Guidelines for drinking-water quality. 2004.

5. Gupta VK, Nayak A, Agarwal S, et al. Removal of Ni (II) ions from water using scrap tire. J Mol Liq. 2014;190:215-22.

6. Saeidi N, Parvini M, Niavarani Z. High surface area and mesoporous graphene/activated carbon composite for adsorption of Pb (II) from wastewater. J Environ Chem Eng. 2015;3(4): 2697–706.

7. Nieto-Márquez A, Pinedo-Flores A, Picasso G, et al. Selective adsorption of Pb^{2+}, Cr^{3+} and Cd^{2+} mixtures on activated carbons prepared from waste tires. J Environ Chem Eng. 2017;5(1): 1060–7.

8. Patel H. Fixed-bed column adsorption study: a comprehensive review. Appl Water Sci. 2019;9(3):1–17.

9. Razi MAM, Hishammudin MNAM, Hamdan R. Factor affecting textile dye removal using adsorbent from activated carbon: A review. In: MATEC Web of Conferences. EDP Sciences.2017; p. 06015.

10. Galindo LSG, Almeida Neto AF de, Silva MGC da, et al. Removal of cadmium (II) and lead (II) ions from aqueous phase on sodic bentonite. Mater Res. 2013;16:515–27.

11. Wang X, Zhang Z, Sun R, et al. High-efficiency removal of low-concentration Hg (II) from aqueous solution by bentonite nanocomposite: Batch and fixed-bed column adsorption study. Sep Sci Technol. 2021;56(13):2204–16.

12. Al-Malack MH, Dauda M. Competitive adsorption of cadmium and phenol on activated carbon produced from municipal sludge. J Environ Chem Eng. 2017;5(3):2718–29.

13. Al-mahbashi N, Kutty SRM, Jagaba AH, et al. Column study for adsorption of copper and cadmium using activated carbon derived from sewage sludge. Adv Civ Eng. 2022;2022:1-11.

14. Yahya MD, Aliyu AS, Obayomi KS, et al. Column adsorption study for the removal of chromium and manganese ions from electroplating wastewater using cashew nutshell adsorbent. Cogent Eng. 2020;7(1):1748470.

15. Letina D, Letshwenyo WM. Investigating waste rock, tailings, slag and coal ash clinker as adsorbents for heavy metals: Batch and column studies. Phys Chem Earth Parts ABC. 2018;105:184–90.

16. Malik DS, Jain CK, Yadav AK. Heavy metal removal by fixed-bed column–a review. ChemBioEng Rev. 2018;5(3):173–9.

17. Shubber MD, Kebria DY. Thermal recycling of bentonite waste as a novel and a low-cost adsorbent for heavy metals removal. J Ecol Eng. 2023;24(5):288–305.

18. Samaka I. Investigate the efficiency of magnetized nanocomposite for sequestration of lead, copper and zinc ions from aqueous solutions [Doctor of Philosophy in Environmental Engineering]. [Iraq]: University of Baghdad; 2018.

19. Zang T, Cheng Z, Lu L, et al. Removal of Cr (VI) by modified and immobilized Auricularia auricula spent substrate in a fixed-bed column. Ecol Eng. 2017;99:358–65.

20. Tsai WC, de Luna MDG, Bermillo-Arriesgado HLP, et al. Competitive fixed-bed adsorption of Pb (II), Cu (II), and Ni (II) from aqueous solution using chitosan-coated bentonite. Int J Polym Sci. 2016;2016.

21. Kaewsichan L, Techato K, Qaisrani ZN, et al. Elimination of selected heavy metals from aqueous solutions using biochar and bentonite composite monolith in a fixed-bed operation. J Environ Chem Eng. 2022;10(1):106993.

22. Malakahmad A, Tan S, Yavari S. Valorization of wasted black tea as a low-cost adsorbent for nickel and zinc removal from aqueous solution. J Chem. 2016;2016.

23. Belhadri M, Mokhtar A, Meziani S, et al. Novel low-cost adsorbent based on economically modified bentonite for lead (II) removal from aqueous solutions. Arab J Geosci. 2019;12(3):1–13.

24. Igberase E, Osifo P, Ofomaja A. Mathematical modelling of Pb^{2+}, Cu^{2+}, Ni^{2+}, Zn^{2+}, Cr^{6+} and Cd^{2+} ions adsorption from a synthetic acid mine drainage onto chitosan derivative in a packed bed column. Environmental Technology. 2018;39(24):3203–20.

25. Liu H, Wang C, Liu J, et al. Competitive adsorption of Cd (II), Zn (II) and Ni (II) from their binary and ternary acidic systems using tourmaline. J Environ Manage. 2013;128:727–34.

26. Dong Y, Lin H. Competitive adsorption of Pb (II) and Zn (II) from aqueous solution by modified beer lees in a fixed bed column. Process Saf

Environ Prot. 2017;111:263–9.

27. Biswas S, Sharma S, Mukherjee S, et al. Process modelling and optimization of a novel Semifluidized bed adsorption column operation for aqueous phase divalent heavy metal ions removal. J Water Process Eng. 2020;37:101406.

28. Futalan CM, Wan MW. Fixed-Bed adsorption of lead from aqueous solution using chitosan-coated bentonite. Int J Environ Res Public Health. 2022;19(5):2597.

29. Karimi M, Shojaei A, Nematollahzadeh A, et al. Column study of Cr (VI) adsorption onto modified silica–polyacrylamide microspheres composite. Chem Eng J. 2012;210:280–8.

30. Al Dwairi R, Omar W, Al-Harahsheh S. Kinetic modelling for heavy metal adsorption using Jordanian low cost natural zeolite (fixed bed column study). J Water Reuse Desalination. 2015;5(2):231–8.

31. Yunnen C, Ye W, Chen L, et al. Continuous fixed-bed column study and adsorption modeling: removal of arsenate and arsenite in aqueous solution by organic modified spent grains. Pol J Environ Stud. 2017;26(4):1847–54.

32. Alamin AH, Kaewsichan L. Adsorption of Pb(II) ions from aqueous solution in fixed bed column by mixture of clay plus bamboo biochar. Walailak J Sci Technol WJST. 2016;13(11):949–63.

33. Abou-Lilah RAK, Badway N, Gamal A, et al. Modeling of the dynamics adsorption of some hazardous elements from aqueous solution onto bentonite-calcium-alginate beads. Al-Azhar Bull Sci. 2021;32(1-A):15–28.

34. Kapur M, Mondal MK. Design and model parameters estimation for fixed–bed column adsorption of Cu(II) and Ni(II) ions using magnetized saw dust. Desalination Water Treat. 2016;57(26):12192–203.

35. Khalfa L, Sdiri A, Bagane M, et al. A calcined clay fixed bed adsorption studies for the removal of heavy metals from aqueous solutions. J Clean Prod. 2021;278:123935.

36. Hayati B, Maleki A, Najafi F, et al. Heavy metal adsorption using PAMAM/CNT nanocomposite from aqueous solution in batch and continuous

fixed bed systems. Chem Eng J. 2018;346:258–70.

37. Gupta S, Jain AK. Biosorption of Ni (II) from aqueous solutions and real industrial wastewater using modified A. barbadensis Miller leaves residue powder in a lab scale continuous fixed bed column. Clean Eng Technol. 2021;5:100349.

38. Malkoc E, Nuhoglu Y. Removal of Ni (II) ions from aqueous solutions using waste of tea factory: Adsorption on a fixed-bed column. J Hazard Mater. 2006;135(1–3):328–36.

39. Lim AP, Aris AZ. Continuous fixed-bed column study and adsorption modeling: Removal of cadmium (II) and lead (II) ions in aqueous solution by dead calcareous skeletons. Biochem Eng J. 2014;87:50–61.